

Atmospheric Dispersion and Deposition of Radionuclides (^{137}Cs and ^{131}I) Released from the Fukushima Dai-ichi Nuclear Power Plant

Soon-Ung Park, Anna Choe, Moon-Soo Park

Center for Atmospheric and Environmental Modeling, Seoul, Korea
Email: supark@snu.ac.kr

Received 2013

ABSTRACT

The Lagrangian Particle Dispersion Model (LPDM) in the $594 \text{ km} \times 594 \text{ km}$ model domain with the horizontal grid scale of $3 \text{ km} \times 3 \text{ km}$ centered at a power plant and the Eulerian Transport Model (ETM) modified from the Asian Dust Aerosol Model 2 (ADAM2) in the domain of $70^\circ \text{ LAT} \times 140^\circ \text{ LON}$ with the horizontal grid scale of $27 \text{ km} \times 27 \text{ km}$ have been developed. These models have been implemented to simulate the concentration and deposition of radionuclides (^{137}Cs and ^{131}I) released from the accident of the Fukushima Dai-ichi nuclear power plant. It is found that both models are able to simulate quite reasonably the observed concentrations of ^{137}Cs and ^{131}I near the power plant. However, the LPDM model is more useful for the estimation of concentration near the power plant site in details whereas the ETM model is good for the long-range transport processes of the radionuclide plume. The estimated maximum mean surface concentration, column integrated mean concentration and the total deposition (wet+dry) by LPDM for the period from 12 March to 30 April 2011 are, respectively found to be $2.975 \times 10^2 \text{ Bq m}^{-3}$, $3.7 \times 10^7 \text{ Bq m}^{-2}$, and $1.78 \times 10^{14} \text{ Bq m}^{-2}$ for ^{137}Cs and $1.96 \times 10^4 \text{ Bq m}^{-3}$, $2.24 \times 10^9 \text{ Bq m}^{-2}$ and $5.96 \times 10^{14} \text{ Bq m}^{-2}$ for ^{131}I . The radionuclide plumes released from the accident power plant are found to spread wide regions not only the whole model domain of downwind regions but the upwind regions of Russia, Mongolia, Korea, eastern China, Philippines and Vietnam within the analysis period.

Keywords: Eulerian Transport Model; Fukushima Nuclear Power Plant; Lagrangian Particle Dispersion Model; Radionuclides of ^{137}Cs and ^{131}I

1. Introduction

On 11 March 2011, an extraordinary magnitude 9.0 earthquake occurred off the Sanriku about 180 km off the Pacific coast of Japan's main island Honshu, at 38.3°N , 142.4°E and followed by a large tsunami [1]. These events caused a station blackout at the Fukushima Dai-ichi nuclear power plant. As a consequence, four of the six Fukushima Dai-ichi nuclear power plants units heavily damaged, and causing a massive discharge of radionuclides into the air and into the ocean.

Fukushima Dai-ichi nuclear power plant consisted of six boiling water reactors lined up directly along the shore. The earthquake triggered the automatic shutdown of the chain reaction in the units 1 to 3 at 05:46 UTC (14:46 JST) on 11 March 2011. Outside power supply was lost and the emergency diesel generators started up. However, the tsunami arrived 50 minutes later and inundated the reactor sites and their auxiliary buildings and caused the total loss of AC power. Cooling of the reactor cores was lost, water levels in the reactor pressure ves-

sels could not be maintained and the cores in all three units that had been under operation, were degraded and partially (or even completely) melted. The hydrogen produced in this process caused major explosions that massively damaged the upper parts of the reactor buildings of units 1 and 3. Damage to the upper parts of the reactor building could be prevented in unit 2, however, a hydrogen explosion were presumably damaged the suppression chamber [2].

During the Fukushima accident period, massive radioactive materials were released to the environment. Several studies have been devoted to estimate released radioactive materials from this accident. Stohl et al. (2012) have made a first guess of released rates based on fuel inventories and then subsequently improved by inverse modeling using the atmospheric transport model and measurement data. The release duration and radioactivity ratios of $^{131}\text{I}/^{137}\text{Cs}$ for the period between 05:00 JST on March 12 to 00:00 JST May 1 in 2011 have been reported [1,3-5]. However, the estimated radionuclides

emission fluxes have been reported to be highly sensitive to the first guess of released rates. The estimated total ^{137}Cs emission flux ranged from 9.1 PBq (JAEA, 2011) for the period of 10-31 March to 36.6 PBq for the period of 10 March to 20 April [2].

To assess air and water contamination levels resulting from the Fukushima accident, as this will be an important consideration when evaluating the various applications to the mitigation measures, the estimates of the dispersion and deposition of radionuclides are required over the site and on the regional scale for a given emission flux. Since the topography in the vicinity of the Fukushima Dai-ichi plant is complex, the Eulerian transport model may not be useful to simulate the detailed concentration and deposition of radionuclides even though it may be reasonable to be used for the simulation of them in a regional scale.

For this purpose the Lagrangian Particle Dispersion Model (LPDM) developed by Park (1998) [6] in the 594 km \times 594 km model domain centered at a power plant and the Eulerian transport model modified from the Asian Dust Aerosol Model 2 (ADAM2) [7] in the model domain of 140 degree longitudinal distance and 70 degree latitudinal distance co-centered with LPDM have been developed to estimate the concentration and deposition of radionuclides released from the nuclear power plant. The LPDM model and the Eulerian Transport Model (ETM) have, respectively, 3 km \times 3 km and 27 km \times 27 km grid spacing of a mesoscale meteorological model with 25 vertical layers. The ETM uses the estimated concentration by LPDM in the Lagrangian model domain as the source for the long-range transport.

The purpose of this study is to estimate concentrations and depositions of radionuclides of ^{131}I in the gas phase and ^{137}Cs in the aerosol phase released from the Fukushima accident for the period from 05:00 JST 12 March to 24:00 JST 30 April 2011 using both LPDM and ETM not only in the eastern Japan but in the regional domain including the Pacific Ocean and Asia.

2. Model Description

2.1. Meteorological Model

The meteorological model used in this study is the fifth-generation mesoscale model of non-hydrostatic version (MM5, PSU/NCAR) in the x, y, and coordinates [8, 9].

The model domains include the LPDM domain (**Figure 1(a)**) and the ETM domain (**Figure 1(b)**) centered by the Fukushima Dai-ichi nuclear power plant (**Figure 1(b)**). The horizontal resolution of ETM is 27 km while that of the LPDM is 3 km with both 25 vertical layers. The simulations with both models have been conducted for the period of 05:00 JST 12 March to 24:00 JST 30 April

2011. The 6 hourly reanalyzed National Center for Environmental Program (NCEP) data are used for the initial and boundary conditions for the MM5 model. The results of the MM5 model are used for ETM. The nested MM5 model in the horizontal resolution of 3 km is used for the LPDM model.

2.2. Eulerian Transport Model (ETM)

The Eulerian transport model (ETM) has been obtained from the modification of the Asian Dust Aerosol Model 2 (ADAM2) [7]. The radionuclide concentrations estimated by LPDM in its domain are used for the source of ETM for the long-range transport of contaminants. The ADAM2 used 11 particle-size bins with near the same logarithmic intervals for the particles of 0.1 - 37 μm in radius [10,11]. This has been changed to the logarithmic size distribution with an aerodynamic mean diameter of 0.4 μm and a logarithmic standard deviation of 0.3 for ^{137}Cs [2], but for ^{131}I , the ADAM2 model has been changed to handle the gas phase contaminants.

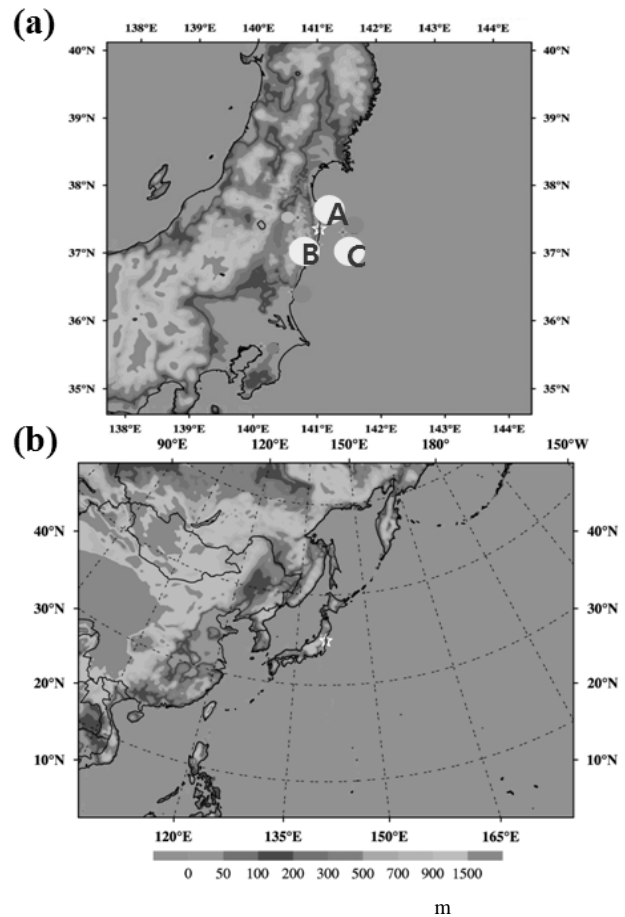


Figure 1. Domain for (a) the Lagrangian particle dispersion model and (b) the Eulerian transport model with the topography. Monitoring sites (A-C) and the Fukushima nuclear power plant site (white star) are indicated.

2.3. Lagrangian Particle Dispersion Model (LPDM)

The LPDM model [6,12-16] is based on conditioned particle concepts in which the conditioned particle is moving with the mean field velocity and the Lagrangian turbulent velocity. The released particle is continuously traced to find its position with time; that is

$$X_i(t + \Delta t) = X_i(t) + (\overline{u_i}(t) + u_i'(t))\Delta t, \quad i=1,2,3 \quad (1)$$

where X_i is the position of the Lagrangian particle, $\overline{u_i}$, and u_i' are the grid scale velocity component that are resolved by the meteorological model and the subgrid scale velocity component respectively, and Δt is the integral time step.

The subgrid scale velocity component is

$$u_i'(t + \Delta t) = R_{L,i}(\Delta t)u_i'(t) + (1 - R_{L,i}(\Delta t))^{1/2}u_i''(t) + \delta_{i,3}(1 - R_{L,i}(\Delta t))w_d \quad (2)$$

where $R_{L,i}$ is the Lagrangian auto correlation coefficient, $\delta_{i,3}$ is the Kronecker delta, u_i'' is the random turbulent velocity component and W_d is the drift correction in vertically in homogeneous turbulence [17]. All necessary parameters and parameterizations are described in details in Park (1998) [6].

The LPDM model takes into account deposition processes; the dry deposition and wet deposition processes. Dry deposition of radionuclides is estimated with the dry deposition velocity, V_d multiplied by concentration of radionuclides near the surface (h_s). The dry deposition velocity, V_d is parameterized with the use of the inferential method [18,19] with taking into account a gravitational settling velocity, V_t for the case of a particle in such a way that

$$V_d = \frac{1}{R_a + R_b + R_c} + V_t \quad (3)$$

where R_a is the aerodynamic resistance, R_b the quasi-laminar sublayer resistance, R_c the surface or canopy resistance and V_t the terminal velocity of a particle. The terminal velocity is given by

$$V_t = \frac{\rho_p g D_p^2}{18\mu} \quad (4)$$

where ρ_p is the density of a particle, g the gravity, D_p the diameter of a particle and μ the dynamic viscosity of air.

In this study, ^{137}Cs is assumed to be in a particle phase with the density of $1,900 \text{ kg m}^{-3}$ and a logarithmic size distribution having an aerodynamic mean diameter of $0.4 \mu\text{m}$ and a logarithmic standard deviation of 0.3 , while ^{131}I is assumed to be in a noble gas phase.

A Lagrangian particle with a hypothetical mass of Q_k positioned at (x_k, y_k, z_k) produces the near surface con-

centration (height of h_s) of

$$C_k(x, y, h_s) = \frac{Q_k e^{-0.693t/\tau}}{(\sqrt{2\pi})^3 \sigma_{kx} \sigma_{ky} \sigma_{kz}} \exp\left[-\frac{(x_k - x)^2}{2\sigma_{kx}^2} - \frac{(y_k - y)^2}{2\sigma_{ky}^2} - \frac{(z_k - h_s)^2}{2\sigma_{kz}^2}\right] \quad (5)$$

where σ_{kx} , σ_{ky} , and σ_{kz} are, respectively the standard deviation of the diffusion distance in the x , y , and z directions associated with the k 's Lagrangian particle, and τ is the half life time of the radionuclide. h_s is assumed to be 5 m above the ground.

The deposition flux due to the k 's Lagrangian particle is

$$F_k = \frac{Q_k V_d e^{-0.693t/\tau}}{(\sqrt{2\pi})^3 \sigma_{kx} \sigma_{ky} \sigma_{kz}} \exp\left[-\frac{(x_k - x)^2}{2\sigma_{kx}^2} - \frac{(y_k - y)^2}{2\sigma_{ky}^2} - \frac{(z_k - h_s)^2}{2\sigma_{kz}^2}\right] \quad (6)$$

Therefore, the total mass deposition of the k 's Lagrangian particle, Q_d is

$$Q_d = \frac{Q_k \Delta t \exp[-0.693 \frac{t + \Delta t}{\tau}] \exp\left[-\frac{(z_k - h_s)^2}{2\sigma_{kz}^2}\right]}{(\sqrt{2\pi})^3 \sigma_{kx} \sigma_{ky} \sigma_{kz}} \int_{-\infty}^{\infty} \int_{-\infty}^{\infty} V_d \exp\left[-\frac{(x_k - x)^2}{2\sigma_{kx}^2} - \frac{(y_k - y)^2}{2\sigma_{ky}^2}\right] dx dy \quad (7)$$

Due to deposition the k 's Lagrangian particle will lose the mass of Q_d after Δt time and results in a reduced mass of k particle after time interval Δt is $Q_k' = Q_k - Q_d$.

The k 's Lagrangian particle is assumed to be totally deposited on the ground if z_k is negative and $|z_k| \geq 3\sigma_{kz}$, otherwise it will be reflected from the ground with the reduced mass of Q_k' .

The wet deposition amounts of radionuclides are determined by the precipitation rate and the averaged concentration in cloud water estimated by the sub-grid cloud scheme followed by the diagnostic cloud model in ADAM2 [6] and the Regional Acid Deposition Model (RADM) version 2.6 [20-22]. The below cloud scavenging process is also included [6].

3. Simulation Results of ^{137}Cs and ^{131}I Concentrations and Depositions

^{131}I is assumed to be in the gas phase with the half-life time of 8.07 days whereas ^{137}Cs is to be in the aerosol phase with the aerodynamic mean diameter of 0.4 m , a logarithmic standard deviation of 0.3 and the half-life time of 30.2 years.

The emission rate of ^{131}I and ^{137}Cs from the Fukushima nuclear power plant accident estimated by [4,5,23] for the period from $05:00 \text{ JST } 12 \text{ March}$ to $24:00 \text{ JST } 30 \text{ April } 2011$ are used in this study and given in **Figure 2**.

The first emission peak of 834 GBq s^{-1} of ^{131}I and 83.4 GBq s^{-1} of ^{137}Cs from 15:30 JST to 16:00 JST 12 March [1] was reported to be related to the hydrogen explosion in reactor unit 1. The highest emission of up to $1,110 \text{ GBq s}^{-1}$ of ^{131}I and 110 GBq s^{-1} of ^{137}Cs during the period of 11:00 JST 14 March to 17:00 JST 15 March 2011 was reported to be relate to the hydrogen explosion in unit 4 and together with the hydrogen explosion in unit 2.

3.1. Simulated ^{131}I and ^{137}Cs Concentrations and Depositions by LPDM

The LPDM model has been employed to simulate radionuclide concentrations and depositions in the domain in **Figure 1(a)**. The Lagrangian particles are released at the rate of one particle per minute at the height of the first σ level (about 18-20 m above the ground) with the appor-tioned mass concentration equivalent to the emission rate in **Figure 2**.

The particle is released starting at 09:00 JST (00:00 UTC) 12 March and ending at 09:00 JST 30 April 2011 for the whole emission period from the Fukushima Dai-ichi nuclear power plant.

The concentration is calculated hourly at each level with the horizontal distance of 1,500 m. The hourly total

deposition (wet and dry) is estimated at each grid with the horizontal distance of 1,500 m.

Figure 3 shows time variations of model simulated daily mean concentrations of ^{137}Cs and ^{131}I with the measured concentrations at 3 sites given in **Figure 1(a)**. Both nuclides are quite well simulated at all sites.

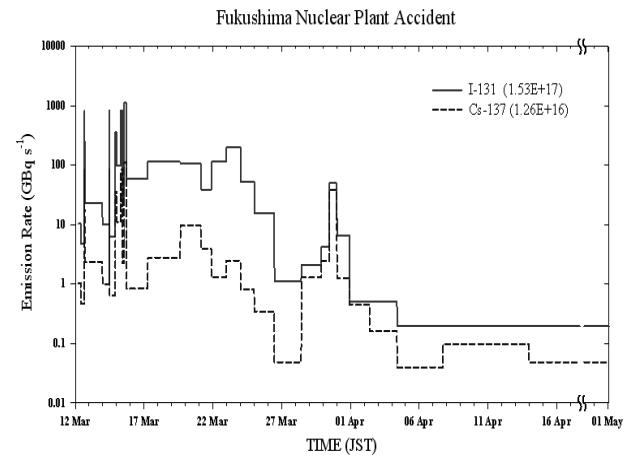


Figure 2. Time variations of emission rate of I-131 (solid line) and Cs-137 (dashed line) from Fukushima nuclear power plant from 12 March to 01 May 2011.

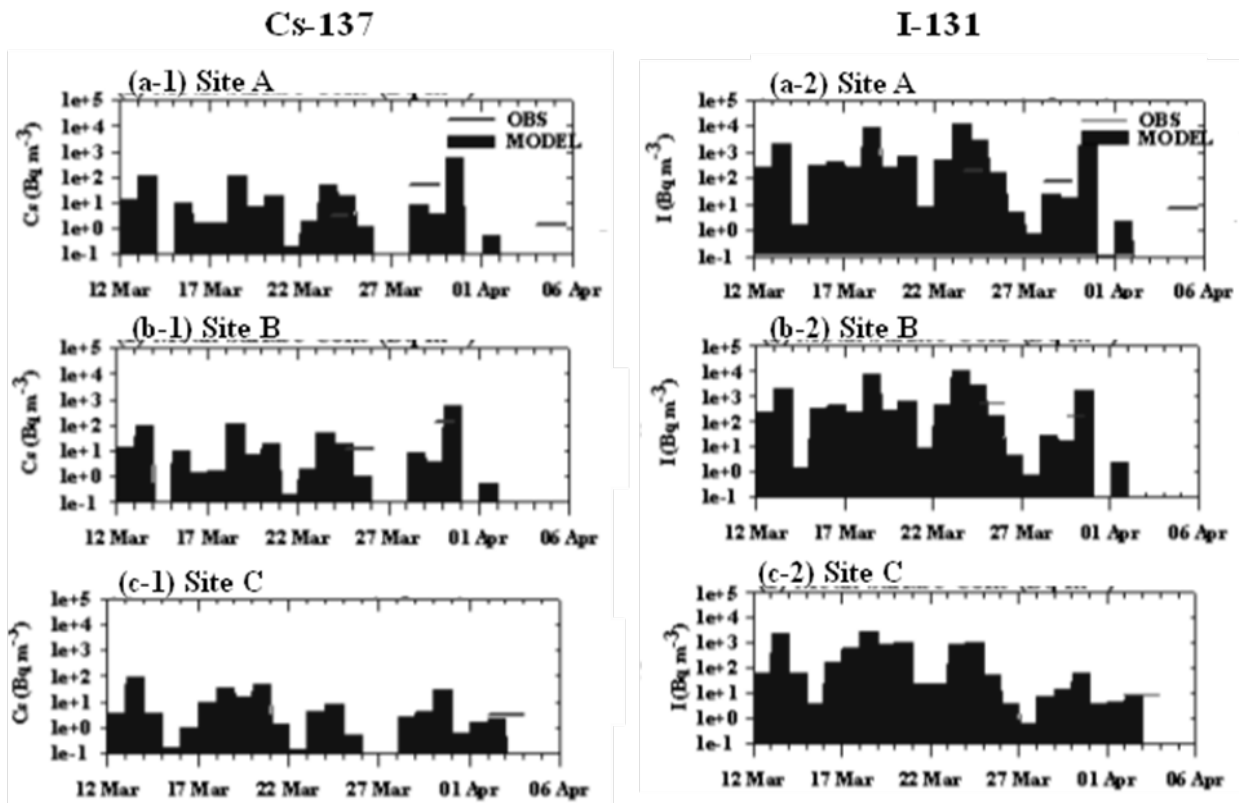


Figure 3. Time variations of model simulated by LPDM daily mean surface concentration (Bq m^{-3}) of (1) Cs-137 and (2) I-131 at (a) site A, (b) site B, and (c) site C for the period from 12 March to 5 April 2011. Observed concentration at each site is shown in with red bars.

Figure 4 shows the horizontal distributions at model simulated mean surface concentration, column integrated mean concentration and total deposition (wet+dry) of ^{137}Cs for the period from 12 March to 30 April 2011. The zone of the mean surface ^{137}Cs concentration exceeding 50 Bq m^{-3} extends northward from the power plant to 38.5N and southward to 35.5N with relative high ^{137}Cs concentrations along the coastline. The maximum surface mean ^{137}Cs concentration of $2.975 \times 10^2 \text{ Bq m}^{-3}$ occurs near the power plant (**Figure 4(a)**). The horizontal distribution pattern of the column integrated mean ^{137}Cs concentration (**Figure 4(b)**) is quite similar to that of the surface mean concentration (**Figure 4(a)**) with the maximum value of $3.7 \times 10^7 \text{ Bq m}^{-2}$ near the power plant. A similar horizontal distribution pattern is also seen in the horizontal distribution of the total deposition of ^{137}Cs . The maximum deposition of $1.78 \times 10^{14} \text{ Bq m}^{-2}$ occurs near the power plant (**Figure 4(c)**).

Figure 5 shows the horizontal distributions of the model simulated surface mean concentration, the column integrated mean concentration, and the total deposition of ^{131}I for the period from 12 March to 30 April 2011. The horizontal distribution pattern of the mean surface ^{131}I concentration (**Figure 5(a)**) is quite similar to that of ^{137}Cs (**Figure 4(a)**) but ^{131}I concentration is much higher than ^{137}Cs due to high emission rate of ^{131}I (**Figure 2**). The area enclosed by the isoline of surface mean ^{131}I concentration of 100 Bq m^{-2} is nearly the same as that of the surface mean ^{137}Cs concentration of 50 Bq m^{-2} (**Figure 4(a)**). The maximum surface mean ^{131}I concentration, and the maximum mean column integrated ^{131}I concentration (**Figure 5(b)**) are, respectively $1.96 \times 10^7 \text{ Bq m}^{-3}$ and $2.44 \times 10^9 \text{ Bq m}^{-2}$ that are 100 times higher than the corresponding values of ^{137}Cs (**Figures 4(a)** and **(b)**). However, the total deposition of ^{131}I with the maximum value of $5.96 \times 10^{14} \text{ Bq m}^{-2}$ (**Figure 5(c)**) is 4 times greater than that of ^{137}Cs , suggesting more effectiveness of the aerosol than the gas for the deposition.

3.2. Simulated ^{131}I and ^{137}Cs Concentrations and Depositions by the Eulerian Transport Model (ETM)

Figure 6 shows the model (ETM) simulated surface mean concentration, the column integrated mean concentration and the total deposition (wet+dry) of ^{137}Cs for the period from 12 March to 30 April 2011.

The emitted ^{137}Cs from the power plant affects all the downwind region of the model domain with some extension toward the upwind region during the analysis period (12 March to 20 April). The high surface mean ^{137}Cs concentration region extends southwestward from Alaska to Philippines with the surface mean maximum concentration of 20 Bq m^{-3} near the power plant (**Figure 7(a)**).

The further upwind extension up to 100°E of the atmospheric loading of ^{137}Cs is seen in **Figure 7(b)** with the maximum column integrated mean ^{137}Cs concentration of $2.78 \times 10^4 \text{ Bq m}^{-2}$ near the power plant.

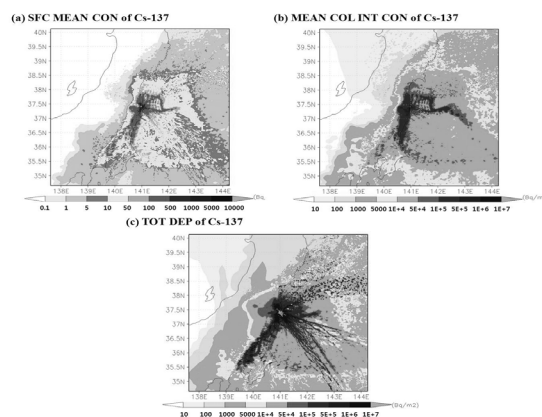


Figure 4. Horizontal distributions of (a) the near surface mean concentration (Bq m^{-3}), (b) the column integrated mean concentration (Bq m^{-2}), and the total deposition (Bq m^{-2}) of ^{137}Cs for the period from 12 March to 30 April 2011.

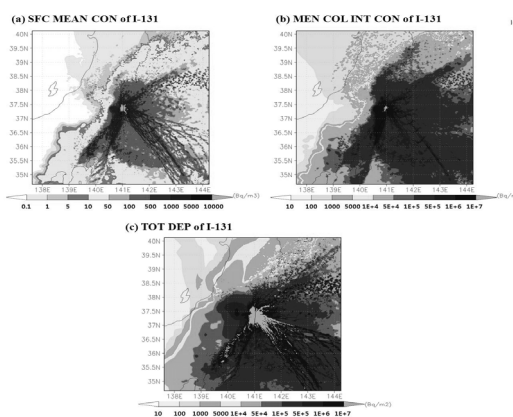


Figure 5. The same as in Figure 4 except for I-131.

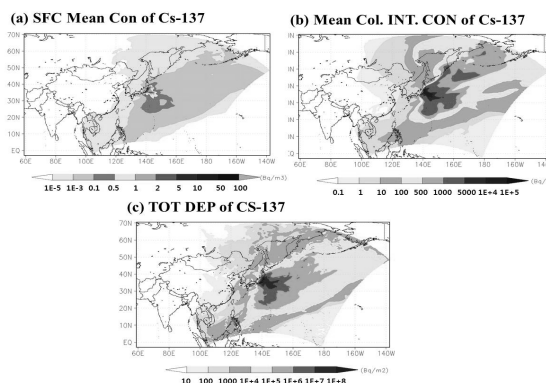


Figure 6. Horizontal distributions of (a) the near surface mean concentration (Bq m^{-3}), (b) column integrated mean concentration, and (c) total deposition of Cs-137 for the period from 12 to 20 April 2011.

Figure 7 shows the model (ETM) simulated surface mean concentration, column integrated mean concentration and total deposition (wet+dry) of ¹³¹I for the period from 12 March to 30 April 2011.

The horizontal distribution patterns of these quantities of ¹³¹I are quite resemble to those corresponding quantities of ¹³⁷Cs (**Figure 6**) but the maximum values are much higher than those of ¹³⁷Cs; The maximum value of the surface mean concentration (**Figure 7(a)**) the column integrated concentration (**Figure 7(b)**) and the total deposition (wet+dry) (**Figure 7(c)**) for ¹³¹I is 851 Bq m⁻³, 1.4 × 10⁶ Bq m⁻² and 8.88 × 10⁵ Bq m⁻², respectively.

To understand the long-range transport process of the radionuclide plume, the daily averaged column integrated ¹³¹I concentration is calculated and presented in **Figure 8** at other day interval from 12 March to 12 April 2011.

The radionuclide plume emitted from the power plant is transported to the downwind region of Alaska and the eastern boundary of the model domain within 4 days (on 15 March).

A well developed low pressure center located at the Bering Sea on 17 March makes the plume to be converged toward the low pressure center and then pushes the plume toward westward over Russia in association with the circulation (21 March). Thereafter the northerlies in association with the developing high pressure system over Siberia push the plume south and southeastward to

Mongolia, East China and Korea (23-27 March).

On the mean time a high pressure system located to the south of the power plant on 19 March makes the emitted radionuclide plume from the power plant to be diverged toward southward to the easterly zone of the subtropical high pressure results in high atmospheric loading of the radionuclide (¹³¹I) zone the along the northern boundary of the subtropical high pressure system that extends southwestward from the northwestern Pacific Ocean to Philippines and Vietnam (19-31 March).

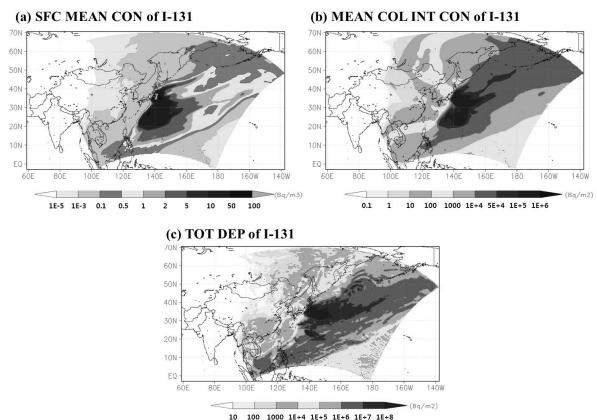


Figure 7. The same as in Figure 6 except for I-131.

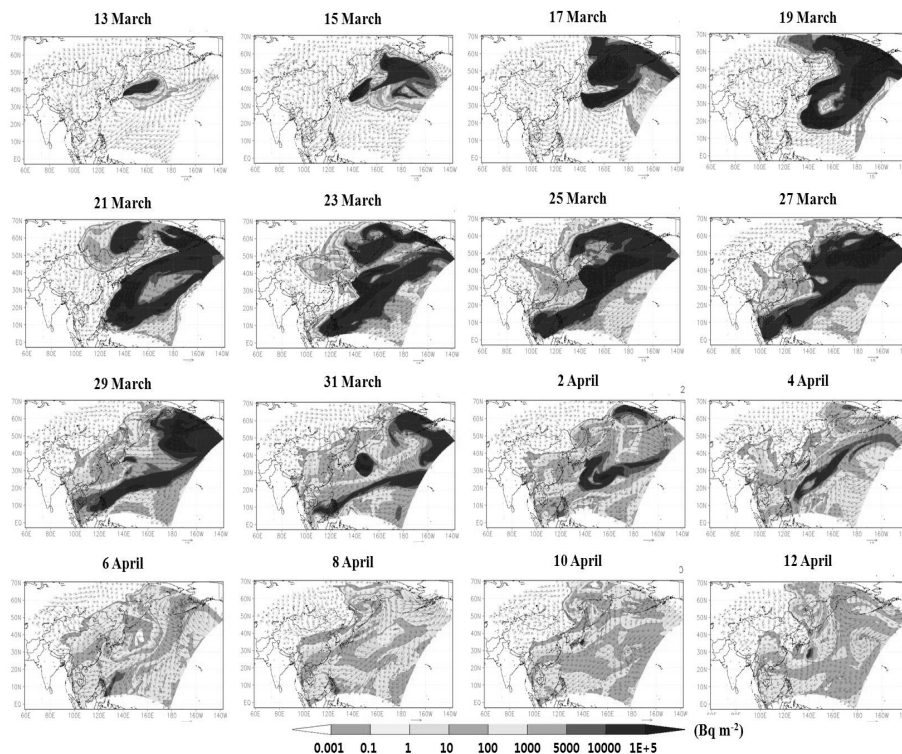


Figure 8. Horizontal distributions of the model simulated daily mean column integrated concentration (Bq m⁻²) of I-131 for every two days starting from 12 UTC 12 March to 12 UTC 12 April 2011.

4. Conclusions

The Lagrangian Particle Dispersion Model (LPDM) in the 594 km × 594 km model domain centered at a power plant with the horizontal grid distance of 3 × 3 km² for meteorological fields and the Eulerian Transport Model (ETM) modified from the Asian Dust Aerosol Model 2 (ADAM2) in the model domain of 140° LON × 70° LAT with the horizontal grid distance of 27 × 27 km² co-centered with LPDM have been developed.

It is found that both models are able to produce the observed concentrations of ¹³⁷Cs and ¹³¹I near the power plant reasonably. The LPDM model yields better results than those of ETM near the power plant. However, the long-range transport processes of the radionuclides are well simulated by the ETM model. Therefore, the presently developed two models are found to be useful for the concentration estimation in the near power plant area by the LPDM model and in the wide region by the ETM model.

The estimated maximum mean surface concentration, mean column integrated concentration and the total deposition by LPDM for the period from 12 March to 30 April are, respectively found to be 2.975 × 10² Bq m⁻³, 3.7 × 10⁷ Bq m⁻² and 1.78 × 10¹⁴ Bq m⁻² for ¹³⁷Cs and 1.96 × 10⁴ Bq m⁻³, 2.24 × 10⁹ Bq m⁻² and 5.96 × 10¹⁴ Bq m⁻² for ¹³¹I. The ETM model result indicates that the radionuclide plume released from the Dai-ichi power plant can affect wide regions not only the whole downwind region of the power plant but the upwind regions including Russia, Mongolia, Korea, the eastern part of China, Philippines and the parts of South East Asia.

The present study mainly pertains to the development of the emergency response modeling system that will be used for the operational model for the accidental releases. Further verification of the model with measured data is required to be used as an operational model.

5. Acknowledgements

This work was funded by the Korea Meteorological Administration Research and Development program under Grant CATER 2012-2050.

REFERENCES

- [1] K. Tanaka, Y. Takahashi, A. Sakaguchi, M. Umeo, S. Hayakawa, H. Tanida, T. Saito and Y. Kanai, "Vertical Profiles of Iodine-131 and Cesium-137 in Soils in Fukushima Prefecture Related to the Fukushima Daiichi Nuclear Power Station Accident," *Geochemical Journal*, Vol. 46, 2012, pp. 73-76.
- [2] A. Stohl, P. Seibert, G. Wotawa, D. Arnold, J. F. Burkhart, S. Eckhardt, C. Tapia, A. Vargas and T. J. Yasunary, "Xenon-133 and Cesium-137 Releases into the Atmosphere from the Fukushima Dai-ichi Nuclear Power Plant: Determination of the Source Term, Atmospheric Dispersion, and Deposition," *Atmospheric Chemistry and Physics*, Vol. 12, 2011, pp. 2313-2343. [doi:10.5194/acp-12-2313-2012](https://doi.org/10.5194/acp-12-2313-2012)
- [3] G. Katata, H. Terada, H. Nagai and M. Chino, "Numerical Reconstruction of High Dose Rate Zones Due to the Fukushima Dai-ichi Nuclear Power Plant Accident", *Journal of Environment Radioactivity*, Vol. 111, 2012, pp. 2-12. [doi:10.1016/j.jenvrad.2011.09.011](https://doi.org/10.1016/j.jenvrad.2011.09.011)
- [4] G. Katata, M. Ota, H. Terada, M. Chino and H. Nagai, "Atmospheric Discharge and Dispersion of Radionuclides during the Fukushima Dai-ichi Nuclear Power Plant Accident. Part I: Source Term Estimation and Local-Scale Atmospheric Dispersion in Early Phase of the Accident," *Journal of Environment Radioactivity*, Vol. 109, 2012, pp. 103-113. [doi:10.1016/j.jenvrad.2012.02.006](https://doi.org/10.1016/j.jenvrad.2012.02.006)
- [5] M. Chino, H. Nakayama, H. Nagai, H. Terada, G. Katata and H. Yamazawa, "Preliminary Estimation of Release Amounts of ¹³¹I and ¹³⁷Cs Accidentally Discharged from the Fukushima Daiichi Nuclear Power Plant into the Atmosphere," *Journal of Nuclear Science and Technology*, Vol. 48, 2011, pp. 1129-1134. [doi:10.1080/18811248.2011.9711799](https://doi.org/10.1080/18811248.2011.9711799)
- [6] S.-U. Park, "Effects of Dry Deposition on Near-Surface Concentrations of SO₂ during Medium-Range Transport," *Journal of Applied Meteorology*, Vol. 37, 1998, pp.486-496. [doi:10.1175/1520-0450\(1998\)037<0486:EODDON>2.0.CO;2](https://doi.org/10.1175/1520-0450(1998)037<0486:EODDON>2.0.CO;2)
- [7] S.-U. Park, A. Choe, E.-H. Lee, M.-S. Park and X. Song, "The Asian Dust Aerosol Model 2 (ADAM2) with the Use of Normalized Difference Vegetation Index (NDVI) Obtained from the Spot4/Vegetation Data," *Theoretical and Applied Genetics*, Vol. 101, 2010, pp. 191-208. [doi:10.1007/s00704-009-0244-4](https://doi.org/10.1007/s00704-009-0244-4)
- [8] D. A. Grell, J. Dudhia, and D. R. Stauffer, "A Description of the 5th Generation Penn State/NCAR Mesoscale Model (MM5), NCAR TECH. Note NCAR/TN-398, p. 117.
- [9] J. Dudhia, D. Grell, Y.-R. Guo, D. Hausen, K. Manning, and W. Wang, "PSU/NCAR Mesoscale Modeling System Tutorial Class Note (MM5 Modeling System Version 2).
- [10] S.-U. Park and H.-J. In, "Parameterization of Dust Emission for the Simulation of the Yellow Sand (Asian dust) Observed in March 2002 in Korea," *Journal of Geophysical Research*, Vol. 108, No. D19, 2003, p. 4618. [doi:10.1029/2003JD003484](https://doi.org/10.1029/2003JD003484)
- [11] S.-U. Park and E.-H. Lee, "Parameterization of Asian Dust (Hwangsa) Particle-Size Distributions for Use in Dust Emission Model," *Atmospheric Environment*, Vol. 38, 2004, pp. 2155-2162. [doi:10.1016/j.atmosenv.2004.01.024](https://doi.org/10.1016/j.atmosenv.2004.01.024)
- [12] R. A. Pielke, M. Arritt, M. Segal, M. D. Moran and R. T. McNider, "Mesoscale Numerical Modeling of Pollutant Transport in Complex Terrain", *Bound-Layer Meteorol*, Vol. 41, 1987, pp. 59-74. [doi:10.1007/BF00120431](https://doi.org/10.1007/BF00120431)
- [13] R. T. McNider, "Investigation of the Impact of Topographic Circulations on the Transport and Dispersion of Air Pollutants," Ph.D. dissertation, University of Virginia, 1981, p. 195.

- [14] T. Yamada, J. Kao, and S. Bunker, "Airflow and Air Quality Simulations over the Western Mountaineous Region with a Four-Dimensional Data Assimilation Technique," *Atmospheric Environment*, Vol.23, 1989, pp.539-554. [doi:10.1016/0004-6981\(89\)90003-6](https://doi.org/10.1016/0004-6981(89)90003-6)
- [15] W. L. Physick, and D. J. Abbs, "Modeling of Summer-time Flow and Dispersion in the Coastal Terrain of Southeastern Australia," *Monthly Weather Review*, Vol.119, 1991, pp.1014-1030. [doi:10.1175/1520-0493\(1991\)119<1014:MOSFAD>2.0.CO;2](https://doi.org/10.1175/1520-0493(1991)119<1014:MOSFAD>2.0.CO;2)
- [16] F. B. Smith, "Conditioned particle motion in a homogeneous turbulent field," *Atmospheric Environment*, Vol.2, 1968, pp.491-508. [doi:10.1016/0004-6981\(68\)90042-5](https://doi.org/10.1016/0004-6981(68)90042-5)
- [17] B. J. Legg, and M. R. Raupach, "Markov-Chain Simulations of Particle Deposition in Homogeneous Flows: The Mean Drift Velocity Induced by a Gradient in Eulerian Velocity Variance", *Bound.-Layer Meteor.*, Vol.24, 1982, pp.3-13. [doi:10.1007/BF00121796](https://doi.org/10.1007/BF00121796)
- [18] M. L. Wesely, "Parameterization of Surface Resistances to Gaseous Dry Deposition in Regional-Scale Numerical Models," *Atmospheric Environment*, Vol.23, 1989, pp.1293-1304. [doi:10.1016/0004-6981\(89\)90153-4](https://doi.org/10.1016/0004-6981(89)90153-4)
- [19] M. L. Wesely and B. B. Hicks, "Some Factors that Affect the Dispersion Rates of Sulfur Dioxide and Similar Gases on Vegetation", *Journal of Air Pollution Control Association*, Vol.27, 1977, pp.1110-1116. [doi:10.1080/00022470.1977.10470534](https://doi.org/10.1080/00022470.1977.10470534)
- [20] C. J. Walcek, and G. R. Taylor, "A Theoretical Method for Computing Vertical Distributions of Acidity and Sulfate Production within Cumulus Clouds," *J. Atmos. Sci.*, 43, 1986, pp.339-355. [doi:10.1175/1520-0469\(1986\)043<0339:ATMFCV>2.0.CO;2](https://doi.org/10.1175/1520-0469(1986)043<0339:ATMFCV>2.0.CO;2)
- [21] J. S. Chang, R. A. Brost, I. S. A. Isaksen, S. Madronich, P. Middleton, W. R. Stockwell and C. J. Walcek, "A Three-Dimensional Eulerian Acid Deposition Model: Physical Concepts and Formulation," *Journal of Geophysical Research*, Vol. 92, 1987, pp. 14681-14700. [doi:10.1029/JD092iD12p14681](https://doi.org/10.1029/JD092iD12p14681)
- [22] R. L. Dennis, J. N. McHenry, W. R. Barchet, F. S. Binkovski and D. W. Byun, "Correcting RADM's Sulfate Underprediction: Discovery and Correction of Model Errors and Testing the Corrections through Comparisons against Field Data," *Atmospheric Environment*, Vol. 27A, No. 6, 1993, pp. 975-997.
- [23] S. Furuta, S. Sumiya, H. Watanabe, M. Nakano, K. Imaizumi, M. Takeyasu, A. Nakada, H. Fujita, T. Mizutani, M. Morisawa, Y. Kokubun, T. Kono, M. Nagaoka, Y. Hiyauma, T. Onuma, C. Kato and T. Kurachi, "Results of the Environmental Radiation Monitoring Following the Accident at the Fukushima Daiichi Nuclear Power Plant," *JAEA-Review*, Vol. 035, 2011, p. 89.